Materials and Design 109 (2016) 123–132

Contents lists available at ScienceDirect

Materials and Design

journal homepage: www.elsevier.com/locate/matdes

Elastic properties of coiled carbon nanotube reinforced nanocomposite: A finite element study

Navid Khani, Mehmet Yildiz, Bahattin Koc *

Faculty of Engineering and Natural Sciences, Sabanci University, Tuzla, Istanbul 34956, Turkey

HIGHLIGHTS

- Modeling and analysis of coiled carbon nanotube (CCNT) reinforced polymer nanocomposites are presented.
- Elastic and shear moduli of CCNT-composites are predicted based on the interphase and geometrical parameters of fillers.
- Comparison of the reinforcing effects of CCNT and SWCNT fillers is presented.

GRAPHICAL ABSTRACT

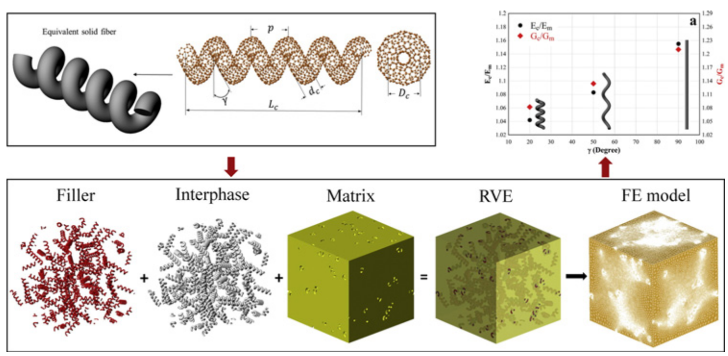

ARTICLE INFO

Article history:
Received 6 March 2016
Received in revised form 28 June 2016
Accepted 29 June 2016
Available online 6 July 2016

Keywords:
Coiled carbon nanotube
Representative volume element
Nanocomposite
Elastic modulus
Finite element analysis

ABSTRACT

This paper presents modeling and analysis of coiled carbon nanotube (CCNT) reinforced polymer nanocomposites. A new algorithmic representative volume element (RVE) generation method and an RVE based finite element analysis are proposed to predict the elastic properties of CCNT nanocomposites. The elastic properties of CCNT polymer nanocomposites are studied with respect to their interphase, volume fraction, orientation, number of coils and geometrical variations such as tube diameter, coil diameter and helix angle using the proposed finite element analysis. The results show that the elastic moduli of randomly and unidirectionally dispersed CCNT nanocomposites decrease when the coil tube or the coil diameter increases. In addition, reinforcement ratio increases by increasing the number of coils. It was also observed that single walled carbon nanotube (SWCNT) fillers have better reinforcement compared to CCNT inclusions with the same volume to surface area ratio.

1. Introduction

In recent years the development of new composite materials is of a great importance in various engineering applications. Numerous research studies have been carried out for improving various aspects of these materials, in particular, their quality and functionality. Different types of nanomaterials as filler have been used to promote the mechanical, thermal and electrical characteristics of nanocomposite materials. Especially, carbon-based nanomaterials including graphene sheets [1–3], carbon nanotubes (CNTs) [4,5], carbon nanocones [6,7], CNT based network [8,9] and coiled CNTs (CCNTs) [10–13] are receiving tremendous attention in the field of nanotechnology.

Among carbon nanostructures, a great deal of interest has been recently focused on CCNTs due to their specific mechanical and electrical properties which stem from the specific helical structures in

* Corresponding author.
E-mail address: bahattinkoc@sabanciuniv.edu (B. Koc).

http://dx.doi.org/10.1016/j.matdes.2016.06.126
0264-1275/

combination with CNTs unique properties [13]. The mechanical properties of CCNTs are studied by a number of researchers. Chen et al. experimentally characterized the mechanics of coiled carbon nanotubes by clamping a CCNT between two AFM cantilevers while a tensile force was applied up to a maximum value. They showed that the spring constant of CCNTs achieved from experimental data are in a good agreement with their analytical model [14]. The optimum conditions for various possible structural configurations of CCNTs were also studied by Chuang et al. [15]. The effective elastic properties of composites of helical fillers in an elastic matrix were studied in [16], by implementing the superposition of fundamental solutions for the matrix and the constitutive equations for the fillers. The geometry of fillers considered in this study was limited to the regular shapes.

Molecular mechanics and molecular dynamics are used to study the elastic, plastic, vibration, spring constants, shear modulus and fracture of CCNTs [17–23]. It is well known that geometry, additive concentrations and properties are the main factors affecting the reinforcement of nanocomposite materials. Wang et al. employed molecular dynamics to differentiate the mechanical properties of the CNTs with the CCNTs where compression, tension, re-compression, re-tension and pullout from a polyethylene matrix were evaluated in [24]. They concluded that CCNTs can be regarded as a suitable filler for tough and lightweight nanocomposites.

The synthesis methods and the applications of CCNTs as fillers in composites were investigated by [25,26]. They reviewed the synthesis procedures of CCNTs and the advantage of a tighter bond with the composite matrix which can result in a variety of engineering applications. Owing to specific geometry of CCNTs, the authors believed that mechanical strength and fracture toughness of the nanocomposite can be substantially enhanced. This unique property can exist even in the absence of any chemical bonding between the CCNT fillers and the matrix.

Several approaches have been used to study the mechanical properties of nanocomposite materials. Since most of the analytical methods for describing the randomly dispersed nanocomposites are not sufficiently precise and they require long times and costly equipment, computational methods are commonly used to analyze the behavior of nanocomposite materials. Multi-scale modeling, molecular dynamics (MD), molecular mechanics (MM) and continuum mechanics are some of the commonly used methods for modeling of nanocomposite materials. However, MD simulation methods are not applicable to every model due to the complexity of model dimension and the extensive time consuming nature of this method. Because of that, most of the MD simulations of nanocomposite materials are restricted to those models which include only a single reinforcement in the matrix of the composite while in reality, nanocomposites can encompass nanofillers with many different shapes, sizes and a wide variety of orientations and arbitrary distributions. Therefore, MD methods are not always suitable for identification and prediction of mechanical properties of nanocomposites. Continuum mechanics; however, is more efficient in characterization of the material properties when the model is more complex. In addition, the knowledge of stress-strain behavior at the boundaries of a representative volume element (RVE) is adequate to accurately characterize the nanocomposites [27]. Finite element analyses (FEA) have been used to determine the mechanical properties of carbon based polymer nanocomposites [28], in particular, the effect of interphase [29–31] and the dispersion of SWCNTs on the properties of nanocomposites [32–37].

A CCNT is a helical form of a CNT (Fig. 1) with several geometrical parameters such as tube diameter d_c, coil diameter D_c, length of coil tube l_c, coiled length L_c, helix angle γ and number of pitch N_c in comparison to a CNT that only has two effective parameters l_s and d_s. When used as a filler, all of these geometrical parameters could affect the overall mechanical properties of a nanocomposite. A recently published study [24–26] showed that composites reinforced by CCNTs would be good potential candidates for lightweight and tough nanocomposites. To the best of our knowledge, there is no numerical study to evaluate effective mechanical properties based on different morphology and random distribution of CCNT inside polymer nanocomposite. Thus, we are presenting a numerical study based on FE analysis to investigate the effect of different geometrical and intrinsic parameters of CCNTs incorporated in a polymer matrix. To determine whether CCNTs could be considered as an alternative to CNTs in polymer nanocomposites for their mechanical properties, we developed an algorithm to compare the effect of changing filler geometry from the case of SWCNTs to CCNTs. Our proposed model is capable of including interphase effect of polymer/CCNTs in determination of the mechanical response of the system.

In Section 2, an RVE generation algorithm is presented to construct the FE model of randomly dispersed SWCNTs and CCNTs in a polymeric composite. The effective mechanical properties of the designed nanocomposites are evaluated using the developed FEA by changing their filler geometry. Section 3 presents the results obtained from analysis of the models. Our conclusive remarks of the developed study are presented in Section 4.

2. Nanocomposite modeling

2.1. RVE construction

This research work is aimed to evaluate the elastic properties of CCNT nanocomposites by considering their volume fraction, geometry and orientation of CCNTs. A finite element analysis is developed as a computational framework for this study with the following steps: (i)

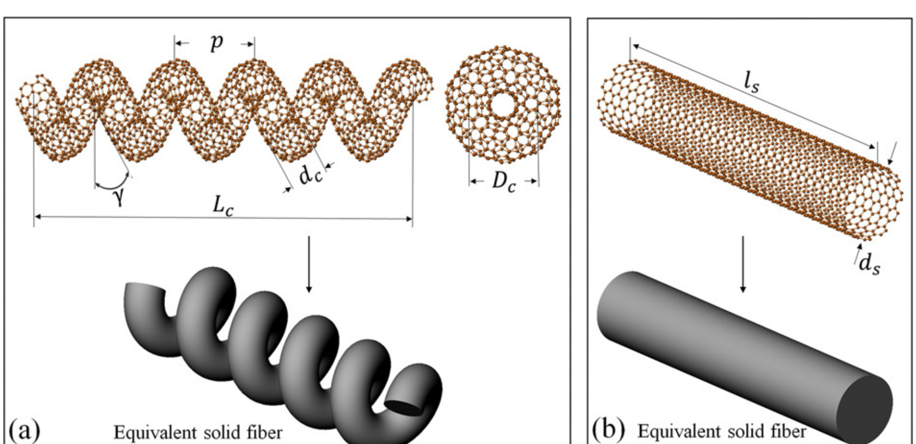

Fig. 1. (a) geometrical parameters and equivalent solid fiber model of a CCNT (b) geometrical parameters and equivalent solid fiber model of a CCNT.

modeling RVEs with a custom algorithm in a Computer Aided Design (CAD) system (ii) generating an ANSYS-APDL script file by using the developed algorithm, (iii) constructing the RVE model in ANSYS-APDL and exporting the model to ANSYS workbench to mesh the generated RVE, and (iv) importing FE model to ANSYS-APDL to analyze and evaluate the results.

An algorithm in CAD environment has been developed for generating CNT and CCNT networks inside a cubic-shaped volume element. Fig. 2 shows the flowchart of the developed algorithm for constructing RVEs with randomly distributed nanofillers.

Modeling of random CNTs and CCNTs inside the polymer matrix is based on a modified Random Sequential Adsorption (RSA) algorithm which is commonly used for short fiber composite analysis [38].Number of fillers, N_c have been selected by a sensitivity analysis that will be explained in results and discussion Section 3.1 and the size of RVE are calculated based on volume fraction, size and number of fillers. The algorithm (Fig. 2) is used for generating a representative volume element (RVE) by stepwise addition of cylindrical nanofibers with randomly generated start point and a specified length. To determine the direction of each fiber in 3D space, a vector was randomly generated. To avoid any intersection between nanofillers, a collision detection algorithm is also used. Hence, a newly generated candidate fiber is accepted if it does not intersect with any previously generated fillers. To create the RVE with appropriate volume fraction and also preserving periodic RVE, parts of the fillers which go beyond the boundaries of the RVE, are moved to the appropriate opposite faces of RVE and again are checked for any intersections. For CCNT fillers, the procedure is the same except the nanofillers' geometry is changed to CCNTs. To generate random CCNT fillers, a parametric helix equation along a random direction vector is generated first. The generated helix is then evaluated with 200 points as shown in Fig. 3. Finally, a B-spline curve is fitted through the points to generate a parametric curve model. It should be noted that ANSYS-APDL only support B-spline curve and the maximum series of points for curve fitting can be at most 200. At the start point of the helix B-spline curve, a circular edge with a dimeter d_c is swept along the curve to generate a CCNT solid filler as shown in Fig. 3.

2.2. Properties and continuum finite element modeling of nanocomposite

Several studies have been reported that SWCNT can be assumed as a truss, shell, equivalent continuum model [32,37] and an equivalent solid fiber model [31,32,37]. The CNTs are not generally isotropic materials and their mechanical behaviors differ in axial and transverse directions. However, isotropic material models can give a reasonable approximation. Many researchers used isotropic model in their studies in general [37] and modeling of nanocomposite materials in particular [28,32]. The former has been proved that the isotropic models also provide reasonable outcomes comparable with experimental data, especially for small deformations [31], while the latter consideration is reasonably correct for the load-bearing nanocomposites. In this research, an equivalent solid fiber model with isotropic and linear elastic behavior has been used to model SWCNT and CCNT. The elastic modulus is calculated by applying a force to a SWCNT and solid fiber model in an isostrain condition [39]. For the equivalent solid fiber of CCNTs, we assume that the CCNT is a straight SWCNT and the elastic modulus is calculated based on [31]. Fig. 1 demonstrates the effective solid fiber model of a CCNT and SWCNT. The load transfer mechanism between the matrix and the nanofiller is due to the existence of an interphase. Several research studies [30,40,41] have been developed to evaluate the interphase effect on elastic modulus of nanocomposites. The real nature of interface is more complex than perfect bonding between the filler and matrix. Actually, there is an angstrom-scale free space between them and a part of the polymer matrix near the filler shows different behavior than the polymer bulk. However, modeling of free space by FEM would result in the appearance of some singularities in the matrices. In the case of the random dispersion of inclusions, modeling of interphase by considering the free space assumption would be computationally costly. Thus, we assumed a solid continuum model with constant interphase thickness which has a perfect bounding with a filler and polypropylene (PP) matrix [31]. The continuum model can also be used for a polypropylene matrix based on the experimental data reported in [42]. Table 1 shows the mechanical properties assumed for the composite components.

Meshing an RVE with CCNT fillers using ANSYS-APDL is difficult to perform because of the mesh distortion and tangling. To solve this problem, the generated models are exported to ANSYS workbench first for meshing and then the mesh files are used in ANSYS-APDL environment to solve and analyze the results. Fig. 4(a) shows the different phases of the RVE and the FE model with random network of SWCNT fillers while Fig. 4(b) presents the same model with a random network of CCNT fillers.

In addition to random dispersion of inclusions, in this research the effect of alignment of fillers is also studied for different parameters of

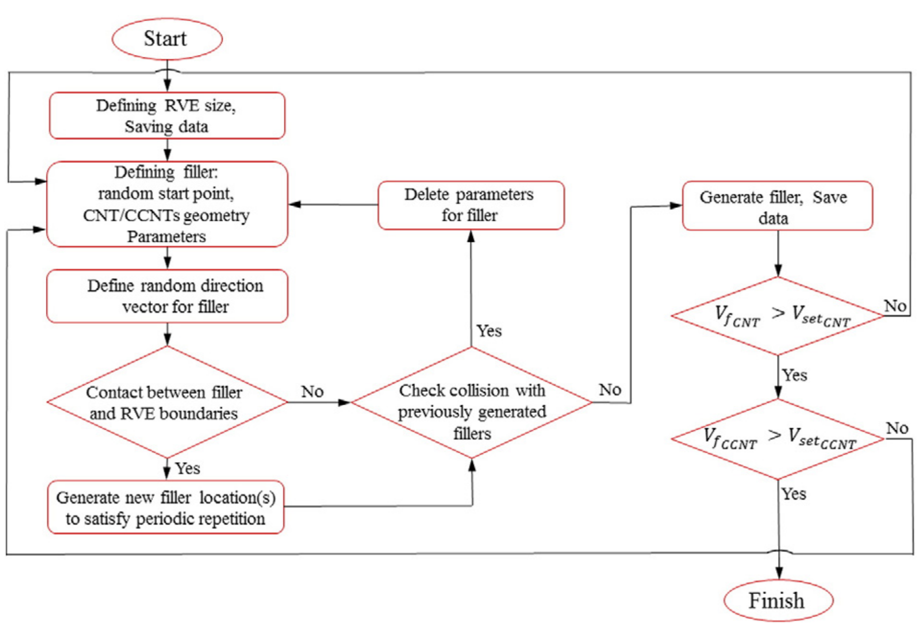

Fig. 2. Flowchart of the generation of RVE.

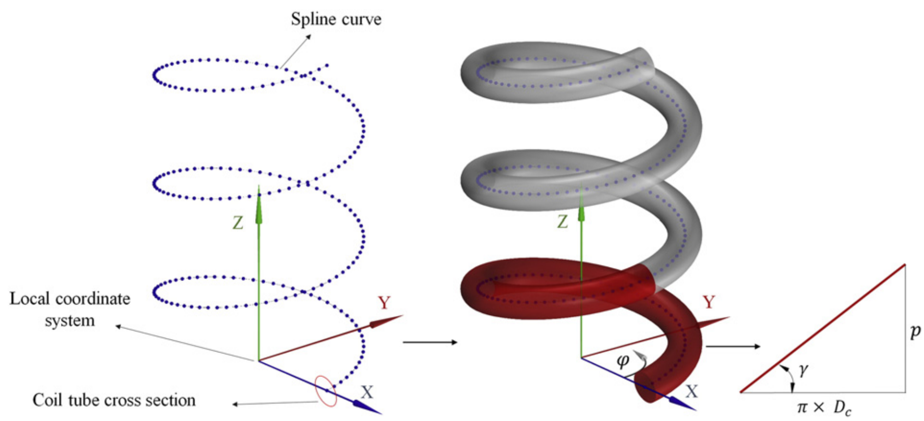

Fig. 3. Generation of CCNT fibers.

CCNTs. Fig. 5 shows a RVE with unidirectional fillers for evaluating longitudinal and transverse elastic modulus of the designed nanocomposites.

2.3. Boundary conditions

The periodic volume element in Fig. 6 allows the implementation of periodic boundary conditions (PBC). Simulation of the real deformation relative to the displacement can be precisely performed by imposing PBC on the volume element. Under these circumstances, the conditions on the displacements or stresses are coupled with the displacements of each point located on the parallel opposite sides. PBC can be written as [43]:

$$^{k^+}u(x) - ^{k^-}u(x) = {}^0\varepsilon \Delta^k x \tag{1}$$

where u and x are the displacement and the position vectors respectively, $^0\varepsilon$ is a constant strain tensor which represents the macroscopic behavior of a volume element and $\Delta^k x$ is a constant distance vector between the pairs of opposite surfaces k^+ and k^-. In order to apply PBC on a volume element, identical meshes are required on the opposite sides where the constraint equations must be applied between the opposite nodal pairs [44].

However, Periodic Boundary Condition is difficult to apply due to its high numerical cost [44]. On the other hand, uniform displacement-traction (orthogonal mixed) BC (MUBC) [45] in most cases cannot give the full elasticity tensor. Pahr and Zyssis [43] developed special MUBC and these BC were applied to a biological random and porous medium. These mixed BC were able to accurately render the tensors of nearly orthotropic samples giving the same overall elastic properties of perfectly orthotropic volume elements as close as periodic BC. Because of this, the method is considered as periodic compatible MUBC (PMUBC). The advantage of PMUBC is that they are also applicable to non-periodic inhomogeneous media and have lower numerical costs as PBC [28].

PMUBC need at least periodic micro geometries of orthotropic or higher elastic symmetry. Pahr and Bohm [46] studied the full elasticity tensor of the composites reinforced with randomly dispersed cylindrical fibers and represented with periodic volume elements by considering PBC and PMUBC. Their work confirmed that results of PMUBC are very close to ones from PBC. In addition, PMUBC are not based on compatible meshes on the parallel faces. Therefore, due to the simplicity in terms of meshing, we have applied PMUBC to the volume elements in this work. Based on notation presented by [43] (see Fig.7), six independent uniform strain load cases are applied to the boundary vectors presented in Table 2 [43]. Stress/strain volume averaging method is used to compute the overall stiffness matrix from the finite element stress/strain results.

Table 1
Mechanical properties of composite component.

	Young's modulus(GPa)	Poisson ratio	Size
CNT	1250	0.3	Diameter = 25 nm
PP	1.98	0.42	Depends on size and number of fillers
Interphase	0.99, 3.96	0.42	Thickness = 20 nm

2.4. Micromechanics

Several micromechanics methods have been used for predicting the elastic properties of composite materials. For verification purpose, the finite element simulation results with SWCNT inclusions are compared to the micromechanical methods based on the Mori–Tanaka and Halpin–Tsai methods. Those methods are explained in the following sections briefly. Also the FEM results (SWCNT and CCNT composite) are checked to see if they meet the classical Hashin-Shtrikman bounds.

2.4.1. Hashin-Shtrikman bounds

Hashin and Shtrikman [47] developed models in which the geometry of the reinforcements was not considered as a limiting factor and the models were based on macroscopical isotropy and quasi-homogeneity of a composite. They assumed a homogeneous and isotropic reference material in which the constituents were dispersed. Taking the stiffness of a reference material with respect to the stiffness of reinforcements, the upper and lower bounds can be given as:

$$K_c^u = K_f + (1-\nu_f)\left[\frac{1}{K_m - K_f} + \frac{3\nu_f}{3K_f + 4G_f}\right]^{-1} \tag{2}$$

$$K_c^l = K_m + \nu_f\left[\frac{1}{K_f - K_m} + \frac{3(1-\nu_f)}{3K_m + 4G_m}\right]^{-1} \tag{3}$$

$$G_c^u = G_f + (1-\nu_f)\left[\frac{1}{G_m - G_f} + \frac{6\nu_f(K_f + 2G_f)}{5G_f(3K_f + 4G_f)}\right]^{-1} \tag{4}$$

$$G_c^l = G_m + \nu_f\left[\frac{1}{G_f - G_m} + \frac{6(1-\nu_f)(K_m + 2G_m)}{5G_m(3K_m + 4G_m)}\right]^{-1} \tag{5}$$

where K_f is the bulk modulus of the filler, G_f is the shear modulus of the filler, K_m is the bulk modulus of the matrix, G_m is the shear modulus of the matrix, K_c is the bulk modulus of the composite, G_c is the shear modulus of the composite, and superscripts "u" and "l" refer to the upper and lower bounds respectively.

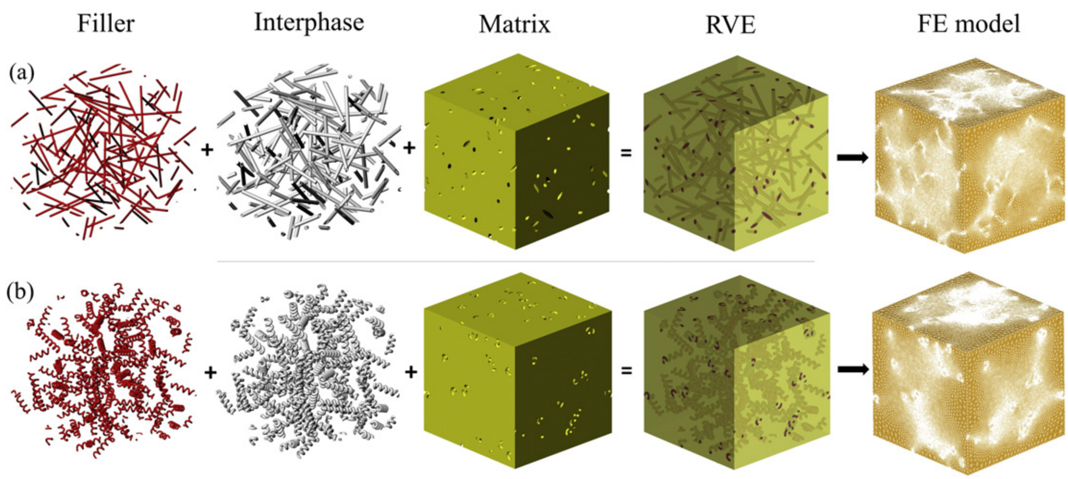

Fig. 4. RVE construction with randomly oriented fillers, interphases, matrix, RVE and FE model (a) CNT-composite; (b) CCNT-composite.

2.4.2. Halpin–Tsai

Halpin and Tsai developed a theory to evaluate the stiffness of composites as a function of aspect ratio [48]. This theory is based on the works of Hermans [49] and Hill [50] where the form of Hill's self-consistent theory was generalized by considering a single fiber incorporated in a cylindrical matrix that is embedded in an infinite medium. The medium itself was assumed to have average properties of a composite. Halpin and Tsai simplified Herman's' results to analytical form that could be used for a number of reinforcement geometries. The overall composite moduli E_c can be written by:

$$E_c = \frac{1+2\frac{l}{d}\eta\nu_f}{1-\eta\nu_f} \tag{6}$$

$$\eta = \frac{\alpha\frac{E_f}{E_m}-1}{\alpha\frac{E_f}{E_m}+2\frac{l}{d}} \tag{7}$$

where l, d, v_f, and α are the length, diameter, reinforcement volume fraction and the orientation of the inclusions respectively. Also, E_f, E_m, and E_c are the elastic modulus of the reinforcement, polymeric matrix and the composite respectively.

2.4.3. Mori-Tanaka

Mean field micromechanics methods can be very useful for the investigation of the effective mechanical properties of composites. The formulation of the mean field approach depends on the inclusion concentration tensors that make a connection between inclusions' averaged fields in a matrix and the corresponding macroscopic fields. The Mori–Tanaka (MT) approach approximates the behavior of composites

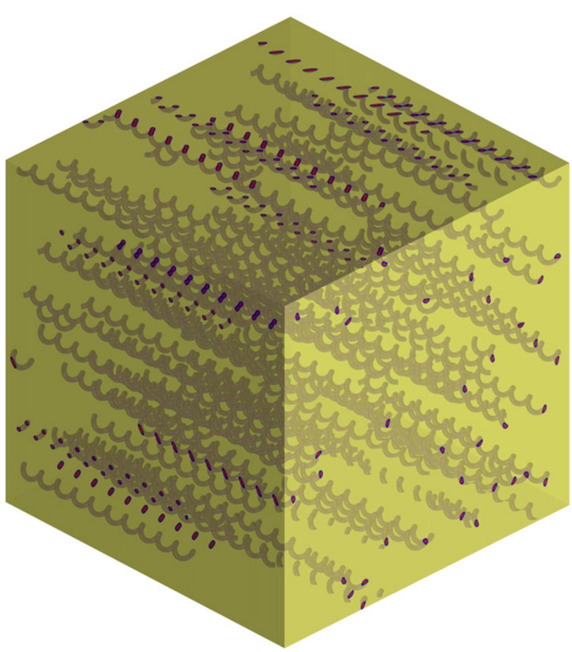

Fig. 5. Composite reinforced by coiled nanotubes with aligned axes.

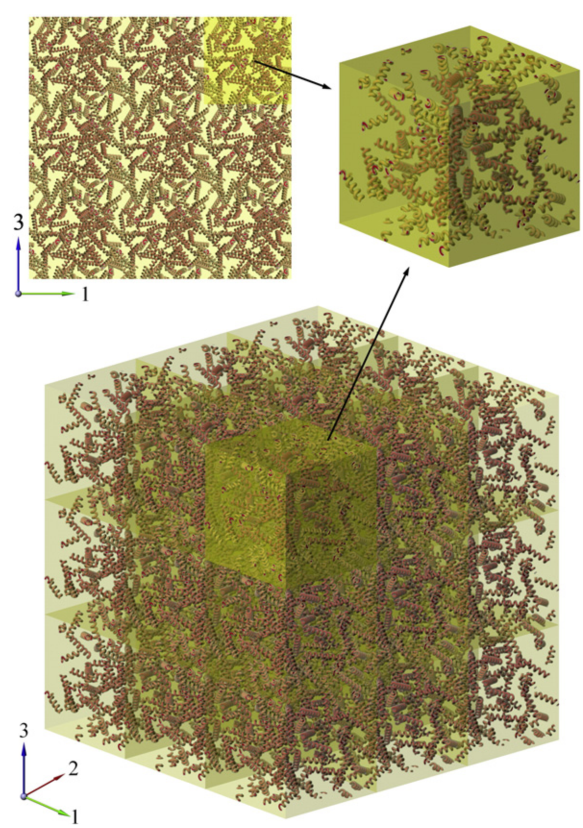

Fig. 6. Periodic volume element for CCNT-composite.

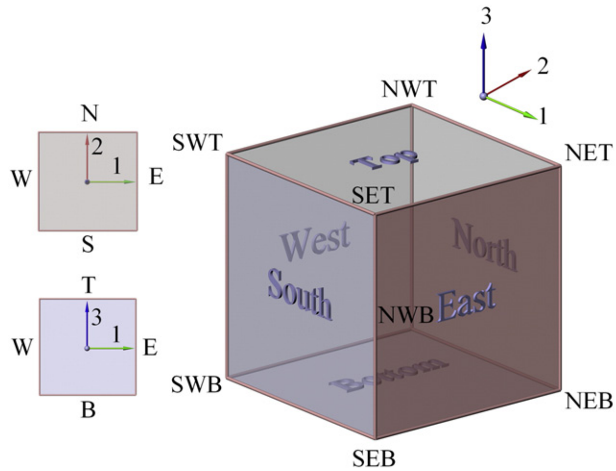

Fig. 7. Notation of the faces for identifying load cases [43].

that contain reinforcements at non-dilute volume fractions via dilute inhomogeneities that are subjected to effective matrix fields rather than the macroscopic fields [51]. These effective fields account for the perturbations caused by all other reinforcements in a mean-field sense [52]. Benveniste [53] expressed the MT methods for elastic composites by the following dual relations:

$$\langle\sigma\rangle^{(i)} = \overline{\boldsymbol{B}}_{dil}^{(i)}\langle\sigma\rangle^{(m)} = \overline{\boldsymbol{B}}_{dil}^{(i)}\overline{\boldsymbol{B}}_{MT}^{(m)}\langle\sigma\rangle \tag{8}$$

$$\langle\varepsilon\rangle^{(i)} = \overline{\boldsymbol{A}}_{dil}^{(i)}\langle\varepsilon\rangle^{(m)} = \overline{\boldsymbol{A}}_{dil}^{(i)}\overline{\boldsymbol{A}}_{MT}^{(m)}\langle\varepsilon\rangle \tag{9}$$

where $\langle\sigma\rangle^{(i)}$, $\langle\sigma\rangle^{(m)}$,$\langle\varepsilon\rangle^{(i)}$ and $\langle\varepsilon\rangle^{(m)}$ are the averaged stress and strain tensors of the inclusion and matrix phases, respectively. $\langle\sigma\rangle$ and $\langle\varepsilon\rangle$ are macroscopic second order stress and strain tensors,$\overline{\boldsymbol{A}}_{dil}^{(i)}$,$\overline{\boldsymbol{B}}_{dil}^{(i)}$ stand for the inclusion dilute and $\overline{\boldsymbol{A}}_{MT}^{(m)}$, $\overline{\boldsymbol{B}}_{MT}^{(m)}$ stand for MT matrices; forth order strain and stress concentration tensors. The Mori-Tanaka stress concentration tensors of the inclusion and matrix can be expressed by:

$$\overline{\boldsymbol{A}}_{MT}^{(i)} = \overline{\boldsymbol{A}}_{dil}^{(i)}\left[(1-\nu_f)\boldsymbol{I} + \nu_f\overline{\boldsymbol{A}}_{dil}^{(i)}\right]^{-1} \tag{10}$$

$$\overline{\boldsymbol{A}}_{MT}^{(m)} = \left[(1-\nu_f)\boldsymbol{I} + \nu_f\overline{\boldsymbol{A}}_{dil}^{(i)}\right]^{-1} \tag{11}$$

where v_f is the inclusion volume fraction and $\boldsymbol{I}$ is the forth order identity tensor. The dilute inclusion concentration tensor,$\overline{\boldsymbol{A}}_{dil}^{(i)}$,can be obtained in analogy to Hill's [54] expression as:

$$\overline{\boldsymbol{A}}_{dil}^{(i)} = \left[\boldsymbol{I} + \boldsymbol{S}\left(\boldsymbol{C}^{(m)}\right)^{-1}\left(\boldsymbol{C}^{(i)} - \boldsymbol{C}^{(m)}\right)\right]^{-1} \tag{12}$$

where $\boldsymbol{S}$ is the Eshelby tensor [55], $\boldsymbol{C}^{(m)}$ and $\boldsymbol{C}^{(i)}$ are the stiffness tensors of matrix and inclusion respectively. Because of the random orientation of particles inside an RVE, the Mori-Tanaka model must represent the integrals from all the directions. For the fourth order tensors, the volume average can be written by [35]:

$$\blacksquare = \frac{1}{4\pi}\int_0^{2\pi}\int_0^{\pi} Q_{mi}Q_{ni}\blacksquare_{mnpq}Q_{pk}Q_{ql}\sin\theta\, d\theta\, d\varnothing \tag{13}$$

Here the braces denote the average over all possible orientations, θ and $\varnothing$ are Euler's angles between the local and global coordinate systems and Q is the corresponding transform matrices. Finally, the Mori–Tanaka macroscopic effective stiffness $\boldsymbol{C}^{(c)}$ tensor of the composite with randomly oriented inclusions can be written by [56]:

$$\boldsymbol{C}^{(C)} = \left[(1-\nu_f)\boldsymbol{C}^{(m)} + \nu_f\ \boldsymbol{C}^{(i)}\overline{\boldsymbol{A}}_{dil}^{(i)}\right]\left[(1-\nu_f)\boldsymbol{I} + \nu_f\overline{\boldsymbol{A}}_{dil}^{(i)}\right]^{-1} \tag{14}$$

3. Results and discussion

In Section 3.1 the results of the sensitivity analysis are provided. The effects of volume fraction and interphase on elastic moduli are discussed in Section 3.2. Finally, the results of a parametric study on the effects of CCNTs geometry on elastic and shear moduli are provided in Sections 3.3 and 3.4. Table 3 lists the effective design parameters and their values which have been used in Sections 3.3 and 3.4.

3.1. RVE size and number of nanofillers

Fig. 8(a) and (b) show the relative elastic modulus of the composite for varying sizes of representative volume element for SWCNT and CCNT fillers with an aspect ratio of 30 and the helix angle of 50° with 1% volume concentration and equal volume size. Six simulations in which the fillers were dispersed under different initial configurations were performed to identify the optimum number of fillers. For a given volume fraction, any increase in the number of fillers will lead to higher RVE sizes. In addition, the error bands will decrease and finally converge to an error less than 1%. Fig. 8(a) clearly shows that the variation error bands are sufficiently small to justify the RVE size for around 60 fillers. In the case of SWCNT, 35 number of fillers are enough to minimize the variation of error bands.

Therefore, the RVE size is a function of the number of fillers and the number of fillers is strongly dependent on the fillers' geometries. Because of the periodic RVEs used, the integrity of CCNTs in a given RVE can decrease dramatically. To compensate this decrease and to achieve more convergent response of the volume element, a higher number of CCNTs are required compare to SWCNTs. In the other words, due to the large diameter of the coil and curvy structure of CCNTs, the probability of division of CCNTs at the edges and the faces of the RVEs into several fragments are higher compared to the case for CNTs. In order to have a reliable simulation, the number of fillers for all SWCNTs and CCNTs are set to 100. More details about the number of fillers and RVE can be found in [57].

Table 2
Matrixes of boundary vectors for six load cases [43].

	Tensile 1			Tensile 2			Tensile 3			Shear 12			Shear 13			Shear 23		
	E	N	T	E	N	T	E	N	T	E	N	T	E	N	T	E	N	T
e_1	$u_1 \neq 0$	$t_1 = 0$	$t_1 = 0$	$u_1 = 0$	$t_1 = 0$	$t_1 = 0$	$u_1 = 0$	$t_1 = 0$	$t_1 = 0$	$t_1 = 0$	$u_1 \neq 0$	$t_1 = 0$	$t_1 = 0$	$t_1 = 0$	$u_1 \neq 0$	$u_1 = 0$	$u_1 = 0$	$u_1 = 0$
e_2	$t_2 = 0$	$u_2 = 0$	$t_2 = 0$	$t_2 = 0$	$u_2 \neq 0$	$t_2 = 0$	$t_2 = 0$	$u_2 = 0$	$t_2 = 0$	$u_2 \neq 0$	$t_2 = 0$	$t_2 = 0$	$u_2 = 0$	$u_2 = 0$	$u_2 = 0$	$t_2 = 0$	$t_2 = 0$	$u_2 \neq 0$
e_3	$t_3 = 0$	$t_3 = 0$	$u_3 = 0$	$t_3 = 0$	$t_3 = 0$	$u_3 = 0$	$t_3 = 0$	$t_3 = 0$	$u_3 \neq 0$	$u_3 = 0$	$u_3 = 0$	$u_3 = 0$	$u_3 \neq 0$	$t_3 = 0$	$t_3 = 0$	$t_3 = 0$	$u_3 \neq 0$	$t_3 = 0$

Table 3
Geometrical features for parametric study.

Case study	CCNTs geometrical features			
	γ (°)	N_c	d_c (nm)	D_c(nm)
γ (°)	20, 50, 90	Varies	25	Varies
N_c	50	10, 15, 20	25	50
d_c (nm)	50	10	15, 20, 25	50
D_c (nm)	Varies	10	25	50, 75, 100

3.2. The effects of volume fraction and interphase

The finite element simulation results for CNT composites are summarized in Fig. 9(a) and compared to the theoretical calculations to verify the simulations. The results show that the theoretical calculations overestimated the elastic modulus compared to the finite element method. It shows that the FE predictions have a similar trend compared to theoretical ones whereas higher values were predicted by the Halpin-Tsai method. The Mori-Tanaka predictions are slightly higher than the FE ones. The intensity of a reinforcement in a composite material is mostly dependent on the filler geometry. This is due to the fact that in composite materials, the force is transferred between matrix and fillers through their contacting surfaces. Therefore, for a constant volume, it is anticipated that the fillers with higher surface areas yield higher reinforcement effects. Because a CCNT is a curvy form of a CNT, we compare the CCNT to the CNT with a same volume to show the effect of changing straight CNT to coiled form of CNT (CCNT) for a better understanding of the CCNT reinforcement. For comparison, Eq. (15) is used to equate the volumes of a SWCNT and CCNT:

$$\frac{\pi \times d_s^2}{4} \times l_s = N_c \times \frac{\pi \times D_c}{\cos\gamma} \times \frac{\pi \times d_c^2}{4} \qquad (15)$$

Taking $D_c = 50$ nm, $d_c = 25$ nm, $\gamma = 50°$, $l_s = 750$ nm and $d_s = 25$ nm in Eq. (15), the number of coils would be equal to 2.41. Thus, considering the same surface area to volume ratio for both SWCNT and CCNT is more meaningful to show their reinforcement effects on nanocomposites. Fig. 9(b) shows the variation of the relative Young's modulus $(^{E_c}/_{E_m})$ of the SWCNT- composite and CCNT- composite with a soft and a hard interphase and the mentioned geometrical parameters. The results show that the reinforcement of SWCNT using the same surface to volume ratio is better than the CCNT reinforcement. Fig. 9(b) also shows that a stiff interphase $(^{E_i}/_{E_m} = 2)$ for both SWCNT and CCNT slightly increases the elastic modulus of composites while a soft interphase $(^{E_i}/_{E_m} = 0.5)$ decreases the reinforcement ratio. It can be concluded that SWCNT composites have a better reinforcement than Coiled SWCNT ones at the same surface to volume ratio.

3.3. Effect of CCNT geometry

This section illustrates the effects of different geometrical parameters of CCNT on the elastic properties of CCNT composites with randomly oriented fillers. A soft interphase and 1% volume fraction are used for all the simulations. Fig. 10(a) shows the variation of different helix angle of a CCNT from coiled filler to perfect straight one; starting from $\gamma = 20°$ to $\gamma = 90°$ by keeping the surface to volume ratio constant. The three designs of fillers in Fig. 10(a) represent geometries with varying D_c, N_c, and γ, while the diameter of coil tube (d_c) and the length of the fillers (l_c) were kept constant. By doing so, the total volume and consequently the surface of each fillers would be the same even by changing the mentioned parameters. The same volume of fillers with different geometries led to the same volume element sizes. As shown in Fig. 10(a), the values of elastic properties increase with an increasing helix angle. In other words, the higher the helix angle, the higher the elastic and shear moduli is for a constant volume of fillers. Fig. 10(b) shows the effect of number of coils on the elastic properties of the composite with a constant surface to volume ratio of the fillers. While keeping all the other parameters the same with $D_c = 50$ nm, $d_c = 25$ nm, $\gamma = 50°$, the number of CCNTs, $N_{c,}$ is changed from 10 to 20. The results in Fig. 10(b) show that by increasing the number of coils in CCNT, the elastic and the shear moduli increased.

Fig. 10(c) shows the effect of diameter of coil tube d_c on elastic moduli by changing d_c from 15 nm to 25 nm and keeping the all the other parameters the same such as $D_c = 50$ nm, $N_c = 10$ and $\gamma = 50°$. The values of the elastic and shear moduli decrease with a larger tube diameter of coils. Moreover, Fig. 10(d) shows the effect of diameter of coil, $D_{c,}$ on the elastic and shear moduli of the CCNT-composite with varying surface to volume ratio of the fillers. Three parameters are kept constant as $d_c = 25$ nm, $N_c = 10$, and $L_c = 1872$ nm while D_c is changed from 50 nm to 100 nm. By keeping L_c constant, γ decreases by increasing D_c.

To physically interpret the results of Fig. 10(c) and (d), it should be noted that the surface to volume ratio for each filler type is the effective parameter in the reinforcement of nanocomposites. Different geometries in Fig. 10(c) represent decrease in surface to volume ratios due to an increase of d_c. Surface to volume ratios changed from 0.267 nm^{-1} to 0.16 nm^{-1} by increasing d_c from 15 to 25 nm.

While the surface to volume ratio of fillers were kept constant in Fig. 10(d), the helix angle decreased from 50° to 30.78° by increasing D_c from 50 to 100 nm. Referring to the results presented in Fig. 10(a), the decrease in elastic and shear moduli was expected by decreasing the helix angle.

3.4. Transversely isotropic CCNT composite

This section illustrates the effect of aligned fillers with different geometrical parameters of CCNT on the longitudinal and transverse elastic properties of CCNT composites. Again, soft interphase and 1% volume

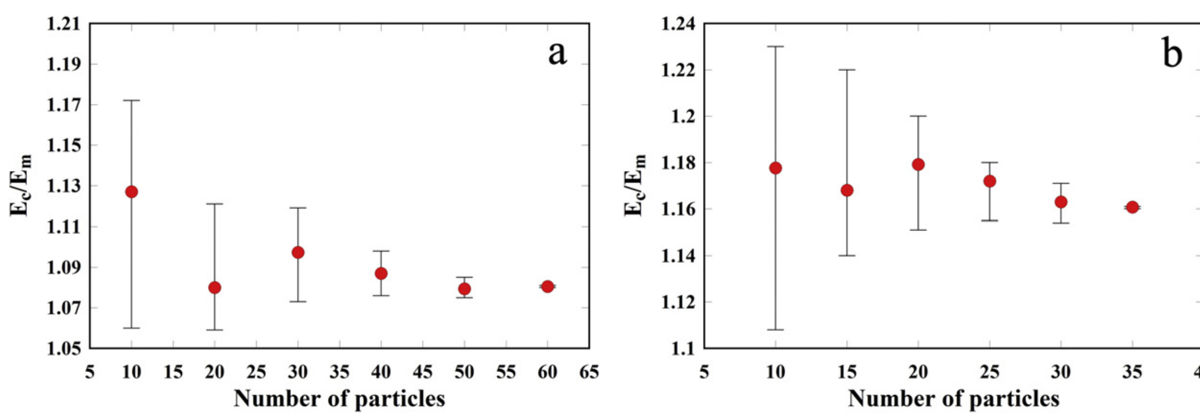

Fig. 8. Evaluation of different numbers of fillers to justify RVE size (a) CCNT- composite; (b) SWCNT- composite.

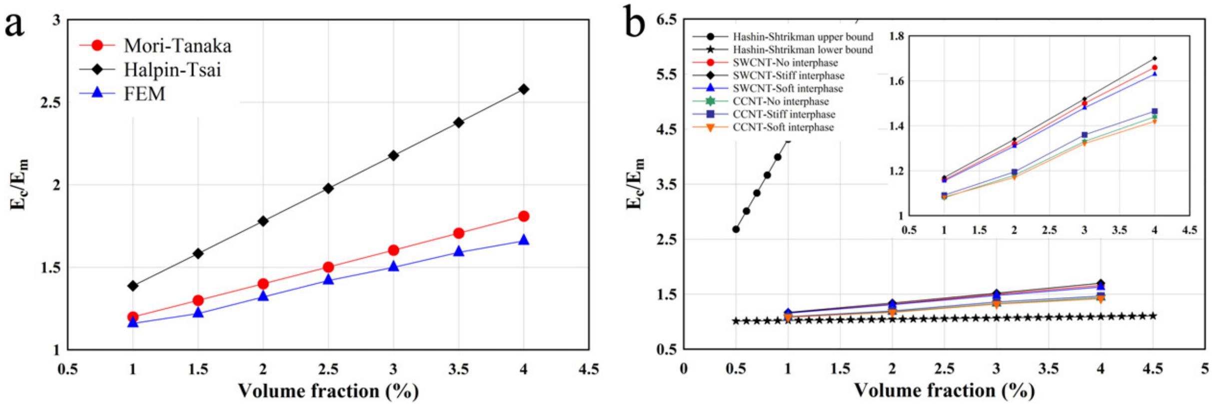

Fig. 9. The effect of volume fraction (a) comparison between analytical models and CNT- composite; (b) The effect of soft and hard interphase reinforcement on CNT and CCNT polymer composites.

fraction are considered for all the simulations. The adjusted parameters are the same with the previous section except the direction of the fillers. Longitudinal and transverse elastic properties of CCNT composites are compared for different parameters as shown in Fig. 11. E_{11} stands for the longitudinal macroscopic Young's modulus and E_{22} is the transverse macroscopic Young's modulus. G_{12} and G_{23} denote longitudinal and transverse macroscopic shear moduli of the composite respectively. The overall trends of longitudinal and transverse elastic properties of CCNT composites are the same in comparison with the randomly dispersed inclusions.

4. Conclusion

In this paper, a computational modeling and a finite element study of elastic properties of CCNT polymer nanocomposites are developed. The developed computational model is used to change the important parameters of CCNT composites such as geometrical variations of tube diameter, coil diameter, helix angle and number of pitch with interphase effect, volume fraction and orientation of reinforcement fillers. The Mori-Tanaka and Halpin-Tsai micromechanics models were used to compare the finite element results of SWCNTcomposites. A perfect bonding has been assumed for the interaction of three different phases of a composite. In addition, the reinforcement effects of CCNT and SWCNT fillers on composite materials are compared. Our conclusion remarks can be drawn as follows:

- While keeping the surface to volume ratio constant, changing the helix angle of randomly dispersed CCNTs from 90 to 0 decreases the effect of reinforcement on the composite. It has also the same effect for the unidirectional inclusions in longitudinal and transverse properties.

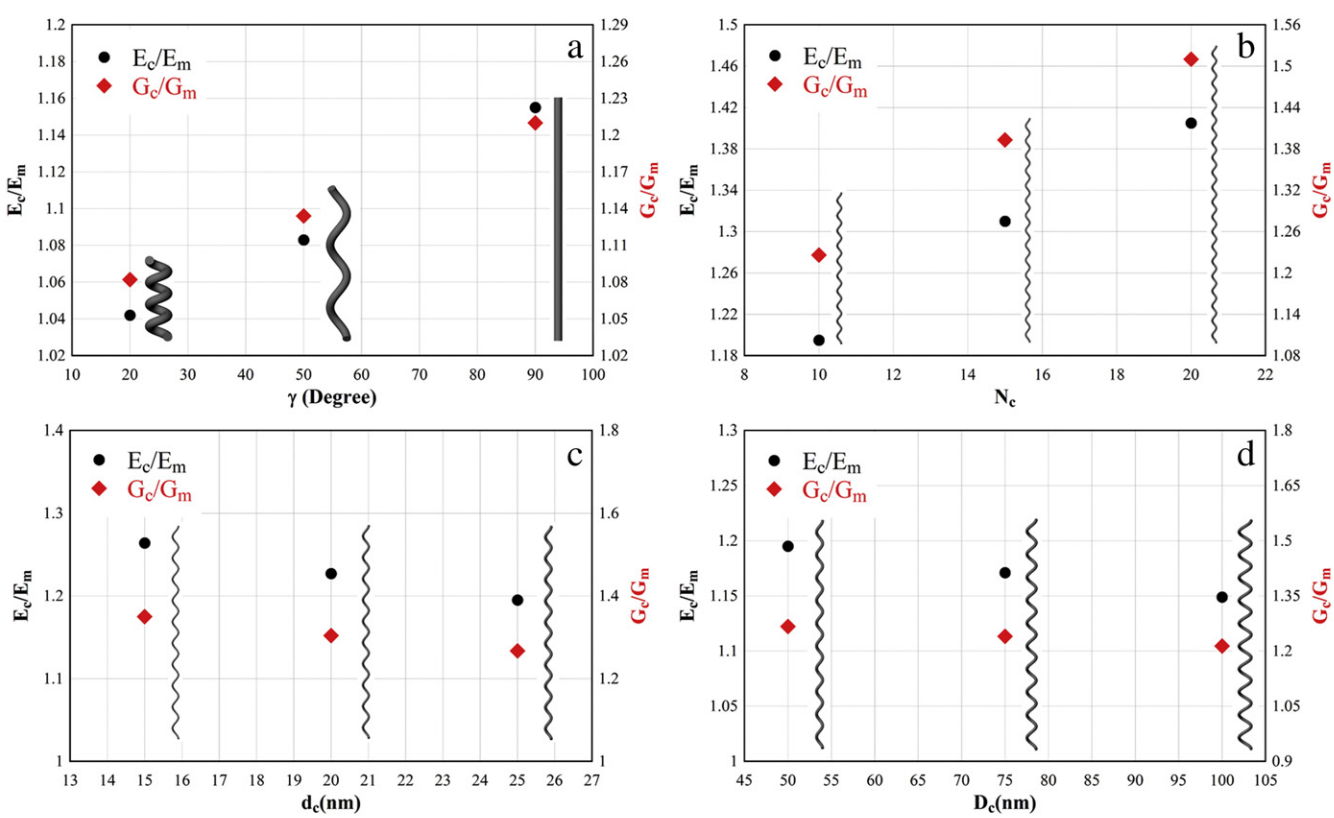

Fig. 10. Effect of different geometrical parameters of the CCNT fillers on the elastics and shear modulus of randomly dispersed composite (a) helix angle; (b) number of coils; (c) coil tube diameter; (d) coil diameter.

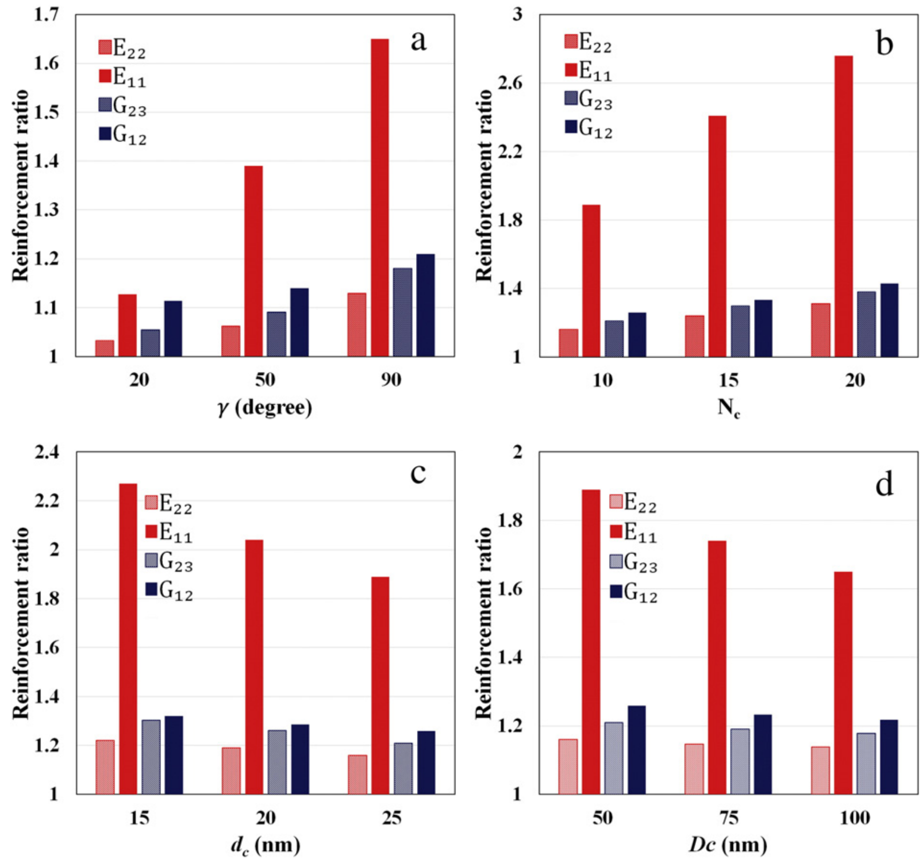

Fig. 11. The effect of different geometrical parameters of CCNT fillers on the Longitudinal and transverse elastic and shear moduli of randomly aligned composites (a) helix angle; (b) number of coils; (c) coil tube diameter; (d) coil diameter.

- Increasing the number of coils leads to a higher elastic and shear moduli for randomly dispersed and unidirectional inclusions.
- The results showed that elastic and shear moduli decrease with the increasing tube and coil diameters.
- The RVE size is sensitive to the geometry of fillers. This means that curved SWCNTs need a larger RVE compared to the SWCNT ones to converge the results.

This work only concentrates on the elastic properties of CCNT polymer nanocomposites. Further studies will be needed to evaluate the plastic behaviors of CCNT composites.

Acknowledgment

This research is supported by The Scientific and Technological Research Council of Turkey (TUBITAK) under grant number 113M491.

References

[1] J.C. Meyer, A.K. Geim, M. Katsnelson, K. Novoselov, T. Booth, S. Roth, The structure of suspended graphene sheets, Nature 446 (7131) (2007) 60–63.
[2] J.S. Bunch, A.M. Van Der Zande, S.S. Verbridge, I.W. Frank, D.M. Tanenbaum, J.M. Parpia, H.G. Craighead, P.L. McEuen, Electromechanical resonators from graphene sheets, Science 315 (5811) (2007) 490–493.
[3] T. Ramanathan, A. Abdala, S. Stankovich, D. Dikin, M. Herrera-Alonso, R. Piner, D. Adamson, H. Schniepp, X. Chen, R. Ruoff, Functionalized graphene sheets for polymer nanocomposites, Nat. Nanotechnol. 3 (6) (2008) 327–331.
[4] W.A. De Heer, A. Chatelain, D. Ugarte, A carbon nanotube field-emission electron source, Science 270 (5239) (1995) 1179–1180.
[5] L. Schadler, S. Giannaris, P. Ajayan, Load transfer in carbon nanotube epoxy composites, Appl. Phys. Lett. 73 (26) (1998) 3842–3844.
[6] N. Yang, G. Zhang, B. Li, Carbon nanocone: a promising thermal rectifier, Appl. Phys. Lett. 93 (24) (2008) 243111.
[7] I.-C. Chen, L.-H. Chen, X.-R. Ye, C. Daraio, S. Jin, C.A. Orme, A. Quist, R. Lal, Extremely sharp carbon nanocone probes for atomic force microscopy imaging, Appl. Phys. Lett. 88 (15) (2006) 153102.
[8] S. Chakrabarti, T. Nagasaka, Y. Yoshikawa, L. Pan, Y. Nakayama, Growth of super long aligned brush-like carbon nanotubes, Jpn. J. Appl. Phys. 45 (7 L) (2006) L720.
[9] K. Liu, Y. Sun, L. Chen, C. Feng, X. Feng, K. Jiang, Y. Zhao, S. Fan, Controlled growth of super-aligned carbon nanotube arrays for spinning continuous unidirectional sheets with tunable physical properties, Nano Lett. 8 (2) (2008) 700–705.
[10] L.Z. Liu, H.L. Gao, J.J. Zhao, J.P. Lu, Superelasticity of carbon nanocoils from atomistic quantum simulations, Nanoscale Res. Lett. 5 (3) (2010) 478–483.
[11] S. Ihara, S. Itoh, J.-i. Kitakami, Helically coiled cage forms of graphitic carbon, Phys. Rev. B 48 (8) (1993) 5643.
[12] H.J.Z.Q.W. Fei, Coiled carbon nanotubes, Prog. Chem. 4 (2009) 008.
[13] L. Liu, F. Liu, J. Zhao, Curved carbon nanotubes: from unique geometries to novel properties and peculiar applications, Nano Res. 7 (5) (2014) 626–657.
[14] X. Chen, S. Zhang, D.A. Dikin, W. Ding, R.S. Ruoff, L. Pan, Y. Nakayama, Mechanics of a carbon nanocoil, Nano Lett. 3 (9) (2003) 1299–1304.
[15] C. Chuang, Y.-C. Fan, B.-Y. Jin, On the structural rules of helically coiled carbon nanotubes, J. Mol. Struct. 1008 (2012) 1–7.
[16] L. Slepyan, V. Krylov, R. Parnes, Helical inclusion in an elastic matrix, J. Mech. Phys. Solids 48 (4) (2000) 827–865.
[17] S.H. Ghaderi, E. Hajiesmaili, Nonlinear analysis of coiled carbon nanotubes using the molecular dynamics finite element method, Mater. Sci. Eng. A 582 (2013) 225–234.
[18] M.M.S. Fakhrabadi, A. Amini, F. Reshadi, N. Khani, A. Rastgoo, Investigation of buckling and vibration properties of hetero-junctioned and coiled carbon nanotubes, Comput. Mater. Sci. 73 (2013) 93–112.
[19] S.-P. Ju, J.-S. Lin, H.-L. Chen, J.-Y. Hsieh, H.-T. Chen, M.-H. Weng, J.-J. Zhao, L.-Z. Liu, M.-C. Chen, A molecular dynamics study of the mechanical properties of a double-walled carbon nanocoil, Comput. Mater. Sci. 82 (2014) 92–99.
[20] C. Feng, K. Liew, P. He, A. Wu, Predicting mechanical properties of carbon nanosprings based on molecular mechanics simulation, Compos. Struct. 114 (2014) 41–50.
[21] S.H. Ghaderi, E. Hajiesmaili, Molecular structural mechanics applied to coiled carbon nanotubes, Comput. Mater. Sci. 55 (2012) 344–349.
[22] J. Wu, S. Nagao, J. He, Z. Zhang, Nanohinge-induced plasticity of helical carbon nanotubes, Small 9 (21) (2013) 3561–3566.
[23] L. Tian, X. Guo, Fracture and defect evolution in carbon nanocoil–a molecular dynamics study, Comput. Mater. Sci. 103 (2015) 126–133.
[24] J. Wang, T. Kemper, T. Liang, S.B. Sinnott, Predicted mechanical properties of a coiled carbon nanotube, Carbon 50 (3) (2012) 968–976.

[25] K.T. Lau, M. Lu, D. Hui, Coiled carbon nanotubes: synthesis and their potential applications in advanced composite structures, Compos. Part B 37 (6) (2006) 437–448.
[26] X.-F. Li, K.-T. Lau, Y.-S. Yin, Mechanical properties of epoxy-based composites using coiled carbon nanotubes, Compos. Sci. Technol. 68 (14) (2008) 2876–2881.
[27] I.E. Afrooz, A. Öchsner, M. Rahmandoust, Effects of the carbon nanotube distribution on the macroscopic stiffness of composite materials, Comput. Mater. Sci. 51 (1) (2012) 422–429.
[28] A.Y. Matveeva, S.V. Pyrlin, M.M. Ramos, H.J. Böhm, F.W. van Hattum, Influence of waviness and curliness of fibres on mechanical properties of composites, Comput. Mater. Sci. 87 (2014) 1–11.
[29] X. Wang, J. Zhang, Z. Wang, S. Zhou, X. Sun, Effects of interphase properties in unidirectional fiber reinforced composite materials, Mater. Des. 32 (6) (2011) 3486–3492.
[30] B. Mortazavi, J. Bardon, S. Ahzi, Interphase effect on the elastic and thermal conductivity response of polymer nanocomposite materials: 3D finite element study, Comput. Mater. Sci. 69 (2013) 100–106.
[31] M.A. Bhuiyan, R.V. Pucha, J. Worthy, M. Karevan, K. Kalaitzidou, Understanding the effect of CNT characteristics on the tensile modulus of CNT reinforced polypropylene using finite element analysis, Comput. Mater. Sci. 79 (2013) 368–376.
[32] J. Huang, D. Rodrigue, Equivalent continuum models of carbon nanotube reinforced polypropylene composites, Mater. Des. 50 (2013) 936–945.
[33] J. Huang, D. Rodrigue, The effect of carbon nanotube orientation and content on the mechanical properties of polypropylene based composites, Mater. Des. 55 (2014) 653–663.
[34] M.M. Shokrieh, R. Mosalmani, A.R. Shamaei, A combined micromechanical–numerical model to simulate shear behavior of carbon nanofiber/epoxy nanocomposites, Mater. Des. 67 (2015) 531–537.
[35] B. Mortazavi, M. Baniassadi, J. Bardon, S. Ahzi, Modeling of two-phase random composite materials by finite element, Mori–Tanaka and strong contrast methods, Compos. Part B 45 (1) (2013) 1117–1125.
[36] M.A. Bhuiyan, R.V. Pucha, J. Worthy, M. Karevan, K. Kalaitzidou, Defining the lower and upper limit of the effective modulus of CNT/polypropylene composites through integration of modeling and experiments, Compos. Struct. 95 (2013) 80–87.
[37] Z. Yuan, Z. Lu, Numerical analysis of elastic–plastic properties of polymer composite reinforced by wavy and random CNTs, Comput. Mater. Sci. 95 (2014) 610–619.
[38] Y. Pan, L. Iorga, A.A. Pelegri, Analysis of 3D random chopped fiber reinforced composites using FEM and random sequential adsorption, Comput. Mater. Sci. 43 (3) (2008) 450–461.
[39] E.T. Thostenson, T.-W. Chou, On the elastic properties of carbon nanotube-based composites: modelling and characterization, J. Phys. D. Appl. Phys. 36 (5) (2003) 573.
[40] M.M.S. Fakhrabadi, N. Khani, Investigation of interphase effects on mechanical behaviors of carbon nanocone-based composites, Mech. Ind. 15 (4) (2014) 287.
[41] K. Spanos, S. Georgantzinos, N. Anifantis, Investigation of stress transfer in carbon nanotube reinforced composites using a multi-scale finite element approach, Compos. Part B 63 (2014) 85–93.
[42] E. Mohammadpour, M. Awang, S. Kakooei, H.M. Akil, Modeling the tensile stress–strain response of carbon nanotube/polypropylene nanocomposites using nonlinear representative volume element, Mater. Des. 58 (2014) 36–42.
[43] D.H. Pahr, P.K. Zysset, Influence of boundary conditions on computed apparent elastic properties of cancellous bone, Biomech. Model. Mechanobiol. 7 (6) (2008) 463–476.
[44] K. Hbaieb, Q. Wang, Y. Chia, B. Cotterell, Modelling stiffness of polymer/clay nanocomposites, Polymer 48 (3) (2007) 901–909.
[45] S. Hazanov, C. Huet, Order relationships for boundary conditions effect in heterogeneous bodies smaller than the representative volume, J. Mech. Phys. Solids 42 (12) (1994) 1995–2011.
[46] D.H. Pahr, H.J. Böhm, Assessment of mixed uniform boundary conditions for predicting the macroscopic mechanical behavior of composite materials(na) 2008.
[47] Z. Hashin, S. Shtrikman, A variational approach to the theory of the elastic behaviour of multiphase materials, J. Mech. Phys. Solids 11 (2) (1963) 127–140.
[48] J. Affdl, J. Kardos, The Halpin-Tsai equations: a review, Polym. Eng. Sci. 16 (5) (1976) 344–352.
[49] J.J. Hermans, Elastic Properties of Fiber Reinforced Materials when the Fibers Are Aligned, Proc. Roy. Academy Amsterdam B, Vol. 70, 1967.
[50] R. Hill, Theory of mechanical properties of fibre-strengthened materials: I. Elastic behaviour, J. Mech. Phys. Solids 12 (4) (1964) 199–212.
[51] T. Mori, K. Tanaka, Average stress in matrix and average elastic energy of materials with misfitting inclusions, Acta Metall. 21 (5) (1973) 571–574.
[52] S. Nogales, H.J. Böhm, Modeling of the thermal conductivity and thermomechanical behavior of diamond reinforced composites, Int. J. Eng. Sci. 46 (6) (2008) 606–619.
[53] Y. Benveniste, A new approach to the application of Mori-Tanaka's theory in composite materials, Mech. Mater. 6 (2) (1987) 147–157.
[54] R. Hill, A self-consistent mechanics of composite materials, J. Mech. Phys. Solids 13 (4) (1965) 213–222.
[55] J.D. Eshelby, The Determination of the Elastic Field of an Ellipsoidal Inclusion, and Related Problems, Proceedings of the Royal Society of London A: Mathematical, Physical and Engineering Sciences, The Royal Society, 1957, pp. 376–396.
[56] G. Weng, The theoretical connection between Mori-Tanaka's theory and the Hashin-Shtrikman-Walpole bounds, Int. J. Eng. Sci. 28 (11) (1990) 1111–1120.
[57] I. Gitman, H. Askes, L. Sluys, Representative volume: existence and size determination, Eng. Fract. Mech. 74 (16) (2007) 2518–2534.